Chapter 8
Adaptive Networks

Huijuan Wang, Stojan Trajanovski, Dongchao Guo and Piet Van Mieghem

We have so far concentrated on networks, which do not change over time. In reality, a network may change over time in an independent process from the epidemic spread. Such networks, where the topology changes according to some rule or pattern, are known as evolving networks. The epidemic threshold in evolving networks has been studied in the past [214, 280]. Adaptive networks possess more complex properties than evolving networks, such that the topology is modified based on epidemic processes.

An adaptive model over the standard SIS model has been considered by Gross et al. [116]. This model is based on fixed probability of an infected nodes to infect and incident susceptible node and a fixed recovery probability of an infected node. Similarly, a link between a susceptible and an infected node is broken with a fixed probability and subsequently, a connection is established between the susceptible node and another susceptible node at random, which is an example of a *rewiring process*. Moreover, Gross et al. [116] have found a bifurcation pattern between the healthy, endemic and bi-stable states in their model. Related model to the model of Gross et al. have been studied by Marceau et al. [177] and Risau-Gusmán [299], while Lagorio et al. [162] have considered a discrete variant of Susceptible-Infected-Recovered (SIR) model in a combination with a rewiring process.

H. Wang (✉) · P. Van Mieghem
Faculty of Electrical Engineering, Mathematics and Computer Science,
Delft University of Technology, Delft, The Netherlands
e-mail: H.Wang@tudelft.nl

S. Trajanovski
Data Science Department, Philips Research, Eindhoven, The Netherlands

D. Guo
School of Computer Science, Beijing Information Science and Technology University,
Beijing, China

E. Altman et al. (eds.), *Multilevel Strategic Interaction Game Models for Complex Networks*, https://doi.org/10.1007/978-3-030-24455-2_8

Separate link-activation and link-deactivation strategies, different from link-rewiring, involving SIR model has been studied by Valdez et al. [261]. This model is discrete and an infected node can infect a susceptible neighbor with a certain probability, otherwise a link is broken for a constant time period. After this time, the link is established again. Following the SIR concept, an infected node becomes susceptible after a fixed time. The model of Valdez et al. [261] differs from the global link rewiring concept of Gross et al. [116] that its dynamic relies on local information and the infectious state of the neighbors of a node. The existence of epidemic threshold was discovered in the model of Valdez et al. [261]. A related model based on the SIS was proposed by Tunc et al. [260].

The majority of these models assume mean-field approximations, thus neglecting the high-order correlations and the local connectivity. The outlook of the final network topology when a meta-stable state is achieved, mean degree [218], degree distribution [116, 290] or concentration of susceptible and infected nodes into loosely connected clusters have not been thoroughly studied.

In this chapter, we will introduce two adaptive spreading processes on networks: the Adaptive Susceptible-Infected-Susceptible (SIS) epidemic model (ASIS) and the adaptive information diffusion (AID) model. The epidemic dynamic in the two models is the some, while the topology dynamic is opposite. In the former, an existing link is broken if one of its end-nodes is infected and the other susceptible; while in the later a link is established between an infected and a susceptible node. Furthermore, a link is established between two susceptible nodes in ASIS model, while an existing link is broken between two such nodes in AID model. ASIS models a process of isolation and distancing from infected nodes, while straightening the susceptible part of the networks, while AID aims to capture the spreading in information and social networks where nodes tend to connect with the information hubs, while the interest in less popular or information lacking nodes diminishes. We will firstly focus on the ASIS model, using both analytical and numerical results to reveal the epidemic threshold, the prevalence and topological features in the metastable-state in relation to ASIS dynamics. Afterwards, we will compare these two models showing that the models have different, but surprisingly not opposite characteristics.

8.1 Adaptive SIS Model

Assuming infection rate β and recovery rate δ, the continuous SIS model drives the epidemic dynamic in ASIS model. The link-dynamic is determined by the adjacency matrix $A(t)$ at time t. The existence of a link between two nodes i and j is specified by $a_{ij}(t) \in \{0, 1\}$ of this adjacency matrix. Each $a_{ij}(t)$ is a Bernoulli random variable, such that $a_{ij}(t) = 1$ with probability $\Pr[a_{ij}(t) = 1]$, while a link absence $(a_{ij}(t) = 0)$ happens with probability $1 - \Pr[a_{ij}(t) = 1]$. The link-breaking and -creating (Fig. 8.1a), visualized in Fig. 8.1a and b, processes are based on viral states of the involved nodes and they are independent from one another. First, if exactly one of nodes i and j is infected and the other susceptible and a link is present between

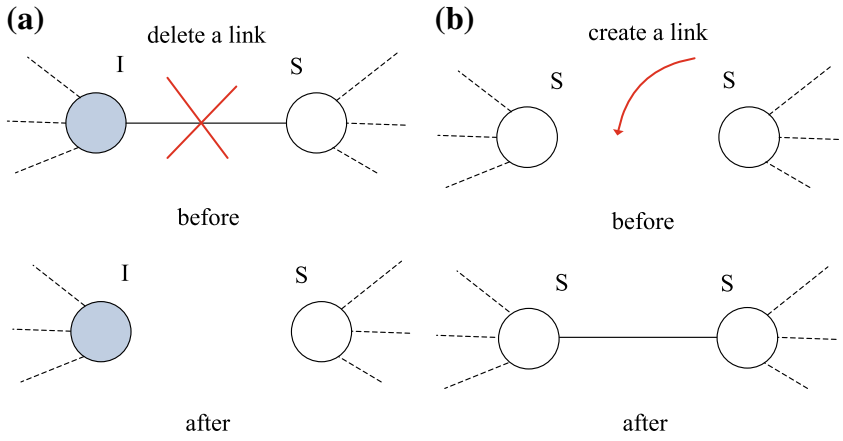

Fig. 8.1 (Color online) Changes of the link states based on the viral states of two nodes. **a** link breaking between a susceptible and an infected node; **b** link creation between two susceptible nodes

them ($a_{ij}(0) = 1$), the link can be deactivated with a Poisson rate ζ. Second, a non existing link can be created between two susceptible nodes i and j with a Poisson rate ξ.

For simplicity and we introduce the following notation:

$$\tilde{t} = t\delta, \quad \tilde{\zeta} = \frac{\zeta}{\delta}, \quad \tilde{\xi} = \frac{\xi}{\delta}, \quad \tau = \frac{\beta}{\delta}, \quad \omega = \frac{2\zeta}{\xi} \tag{8.1}$$

such that τ and ω are the effective infection and link-breaking rates, respectively, while the variable $\tilde{t}$ is the time t scaled by the curing rate δ. For simplicity, in what follows, we will drop $\tilde{}$ notation and continue with these dimensionless parameters. The governing equation of the ASIS dynamics is the following

$$\frac{d}{dt}E[X_i] = E\left[-X_i + (1 - X_i)\tau \sum_{j=1}^{N} a_{ij}X_j\right] \tag{8.2}$$

$$\frac{d}{dt}E[a_{ij}] = a_{ij}(0) \cdot E\left[-\zeta a_{ij}\left(X_i - X_j\right)^2 + \xi\left(1 - a_{ij}\right)(1 - X_i)(1 - X_j)\right] \tag{8.3}$$

How this general model is related to previously introduced ones can be found in [118]. We restrict our analysis in the complete graph K_N in the starting moment $t = 0$, because only for a complete graph K_N, an exact analysis is possible.

8.1.1 The Metastable State of ASIS

The metastable state The meta-stable state is the value of empirically determined time point of the plateau of the average number of infected nodes [62]. The obstacle of this approach is the presence of uncertainty in the choice of the time moment to calculate the value of the meta-stable state value, which depends on the spreading rates and the network topology. On the other hand, the metastable state can be determined by ε-SIS model [272] and finding its stable state. The ε-SIS model [272] is a generalized version of the SIS model, introducing a small self-infection rate $\varepsilon < \frac{\delta}{N}$. This assumption contributes to diminishing the absorbing state and a steady-state is always present for a positive ε. If $\varepsilon = 0$, ε-SIS model boils down to the SIS model. Extending the ε-SIS model with appropriate link dynamics as defined before leads to adaptive ε-SIS model (ε-ASIS model). In such a model and for a small ε, it is possible to calculate the average steady-state values for many metrics, including the number of infected nodes on average or the number of links.

It has been shown [118] that the steady-state in ε-ASIS model resembles the metastable state of the ASIS model.

8.1.2 The Average Metastable-State Fraction of Infected Nodes

The fraction of infected nodes is defined as $Z = \frac{1}{N}\sum_i X_i$, while the average fraction of infected nodes in the metastable state is denoted as $y = E[Z^*]$. Here, we employ the notion of Z^* for the fraction of infected nodes and subsequently, similar is done for other metrics. Assuming a complete graph as an initial topology, we have the following Theorem 8.1.

Theorem 8.1 *For a complete graph K_N as an initial topology and the average metastable-state of infected nodes $y = E[Z^*]$, using (8.2) and (8.3), the following quadratic equation holds*

$$y^2 - 2Vy + H = 0 \tag{8.4}$$

such that

$$V = 1 - \frac{1}{2N} + \frac{\omega - 1}{2\tau N} \tag{8.5}$$

and

$$H = 1 - \frac{1}{N} + Var\left[Z^*\right] - E\left[\frac{1}{N^2}\sum_{j=1}^{N} d_j^*\left(1 - X_j^*\right)\right] \tag{8.6}$$

The solution of the quadratic equation (8.4) is given by

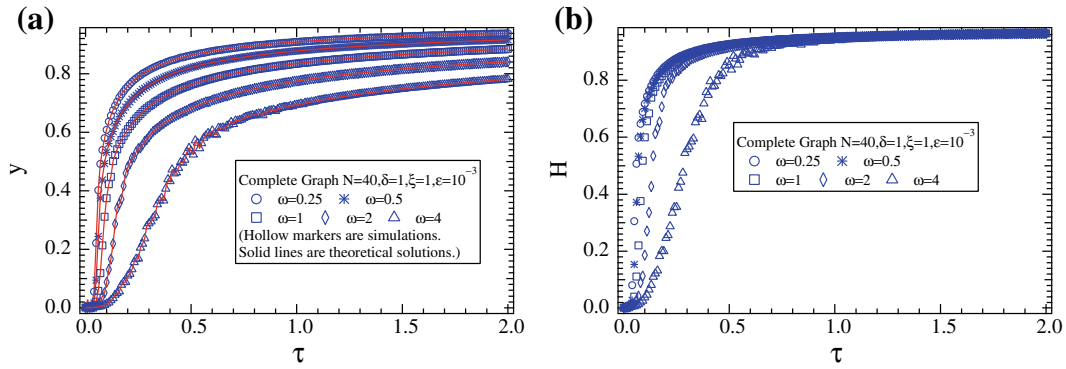

Fig. 8.2 **a** Numerically determined values (in the solid red lines) from (8.7) compared to the simulation results (with blue markers) show a good agreement for the average fraction of infected nodes y in the metastable state as a function of τ. The initial topology is a complete graph. **b** The corresponding values of H in (8.6)

$$y = \left(1 - \frac{1}{2N} + \frac{\omega - 1}{2\tau N}\right)\left(1 \pm \sqrt{1 - \frac{1 - \frac{1}{N} + Var[Z^*] - E\left[\frac{1}{N^2}\sum_{j=1}^{N} d_j^*\left(1 - X_j^*\right)\right]}{\left(1 - \frac{1}{2N} + \frac{\omega-1}{2\tau N}\right)^2}}\right). \quad (8.7)$$

$Var[Z^*]$ is the variance of the fraction of infected nodes, while nodal degree of j is denoted by d_j^*, such that $\frac{d}{dt}E\left[\frac{2L}{\xi} - \frac{(\omega-1)N}{\beta}Z\right] = 0$.

Although the Eq. (8.7) formally has two solution, only one is physically possible. In a case of $\tau \to \infty$ with finite ω, the solution with plus sign in (8.7) is physically valid, while in the opposite case, the solution with minus sign in (8.7) is relevant. If there is no link dynamics i.e. $\omega \to 0$, (8.4) boils down to an equation for a complete graph [60] independent from the time t.

In addition, for several values of effective link-breaking rates ω and given ink-creating rate ξ, Theorem 8.1 has been confirmed by simulations. The solution, given in (8.7), is calculated numerically by applying the values of Var$[Z^*]$ and $E\left[\sum_j d_j^* X_j^*\right]$ that are taken from the simulations. Figure 8.2a show that this solution of (8.7), obtained numerically, is in accordance with the simulation results for multiple cases. The values of H in (8.6) is smaller than 1, and this has been verified in Fig. 8.2b. Figure 8.3a and b depict the behavior of y and H as a function of the rate ω. Additionally, Theorem 8.1 and the fact that $H < 1$ are reaffirmed again. The average fraction of infected nodes in the metastable state decreases as a function of the effective link-breaking rate ω, thus the topology adaptation contributes to the suppression of the virus spread.

Epidemic Threshold

Theorem 8.2 *In ASIS model on K_N, for the epidemic threshold holds*

$$\tau_c(\omega; \xi) = \frac{\omega - 1}{N\left(h(\omega; \xi) - 2 + \frac{1}{N}\right)} \quad (8.8)$$

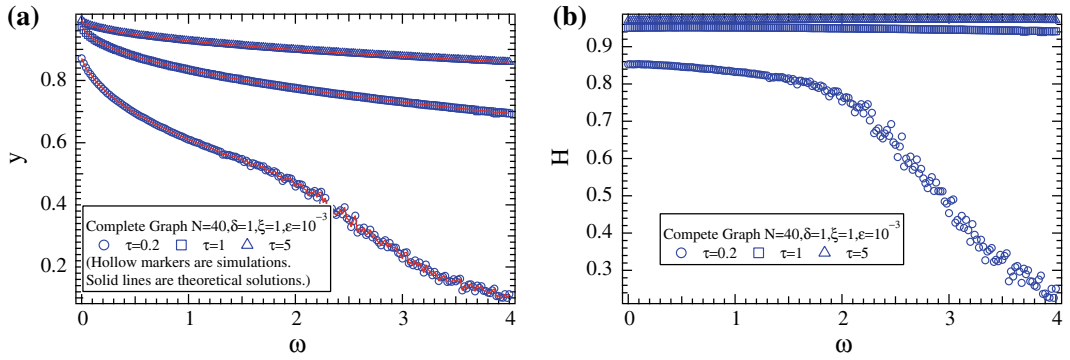

Fig. 8.3 (Color online) **a** Numerically determined values (in the solid red lines) from (8.7) compared to the simulation results (with blue markers) show a good agreement for the average fraction of infected nodes y in the metastable state as a function of ω. The initial topology is a complete graph. **b** The corresponding values of H in (8.6)

such that $h\,(\omega;\xi) = \lim_{y\downarrow 0} \frac{H}{y}$ *is a positive, but slowly changing function such that*

$$1 \leq h\,(\omega;\xi) \leq 2 + \frac{1}{N}\left(\frac{1}{\frac{\partial \tau_c(\omega;\xi)}{\partial \omega}\Big|_{\omega\to\infty}} - 1\right)$$

for all $\omega > 0$ *and* $h\,(1;\xi) = 2 - \frac{1}{N}$.

According to Theorem 8.2, the epidemic threshold τ_c behaves as a linear function in ω since the function $h(\omega;\xi)$ changes very slowly in ω. This trend is mostly noticeable for large ω.

The function $h(\omega;\xi) = \frac{H(\tau_c)}{y_c}$ and the epidemic threshold are obtained experimentally. Figure 8.4b explains that $h(\omega;\xi)$ is slowly changing in ω. In particular, the inset of Fig. 8.4b shows that $h(\omega;\xi)$ is stable and close to a constant for large ω, while Fig. 8.4a depicts that τ_c is close to a linear function in ω. These two observations are in accordance to Theorem 8.2.

8.1.3 Metastable-State Topology

Impact of the Disease Dynamics on the Metastable-State Topology

In this section, we study several topological metrics such as: the modularity (as expressed in [275]), the assortativity [276], the connectivity (expressed as a probability of the that the graph being connected), the average number of components, the biggest component size and the number of links in the metastable state of ASIS. We consider $E[2L^*]/(N(N-1))$ the average number of links in the metastable state scaled by the maximum number of links ($\frac{N(N-1)}{2}$ in a complete

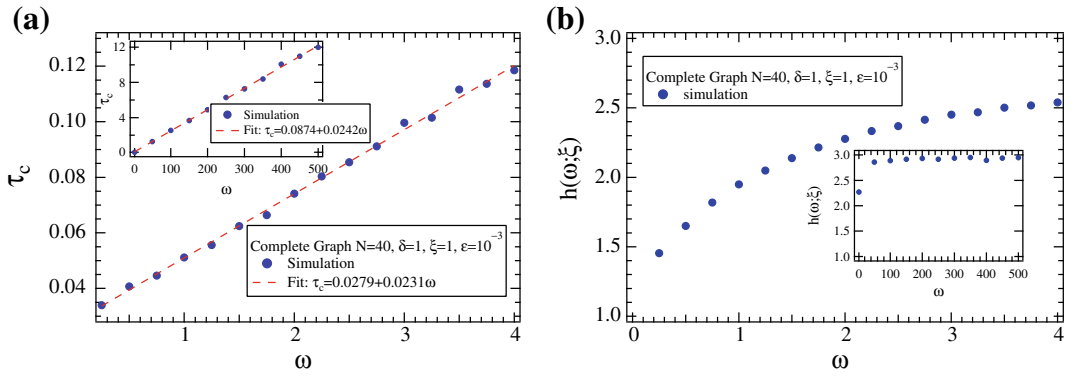

Fig. 8.4 (Color online) **a** Epidemic threshold τ_c as a function of ω for an initial complete graph with 40 nodes. The trend of τ_c for larger values of ω is shown in the inset. Based on the method from Sect. 8.1.2, simulations are conducted and are shown with blue circles. **b** The corresponding function of $h(\omega; \xi)$ in ω. The trend of $h(\omega; \xi)$ for larger values of ω is shown in the inset

graph). $E[2L^*]/(N(N-1)$ in the metastable state has a small value for small τ as shown in Fig. 8.5a. The reason behind is that effective infection rate contributes for the links to break. However, for $E[2L^*]/(N(N-1))$ slowly increases with τ (e.g., $\tau \in [0, 1500]$) as shown in the inset of Fig. 8.5a. The value of $E[2L^*]/(N(N-1))$ could easily reach a maximum value of 1 if τ is very high, because all the nodes will be infected very fast, there will be not enough time for healing or link breaking and subsequently no link will be broken once all are infected. There is also a strong correlation with the number of links with different metrics like the size of the biggest component or the connectivity. For example, the connectivity is shown in Fig. 8.5b, where if $\omega = 2\zeta/\xi > 1$ is high, the network is likely to be disconnected. Moreover for high enough $\omega > 1$, a common phenomena is that the network is partition into one big cluster (component) with almost all the nodes and few components with very small number of nodes. Gross et al. [116] reported that the inclusion of some moderate link-dynamics can introduce correlation in the network, which is also observed in this work. Figure 8.5f shows that the modularity and assortativity demonstrates a strong correlation, which was earlier observed by Van Mieghem et al. [275] in different networks. The process of breaking links contributes to a network separation into two weakly inter-connected components, namely a component of predominantly susceptible node (named as S component) and the other of mostly infected nodes (named as I component). On the other hand, the process of link-creation contributes to strengthening the S component and the connectivity between its nodes. The effect is opposite for the infection and curing rates, where both try to destroy the separation into S and I components. The epidemic and link dynamics are in "persistent competition", for example once the assortativity achieves a maximum value, it starts decreasing due to the increase of the infection rates. This can be observed in Fig. 8.5e. Something similar happens with the modularity (Fig. 8.5f). The presence of S and I components that weakly connected has also been observed in other models [116].

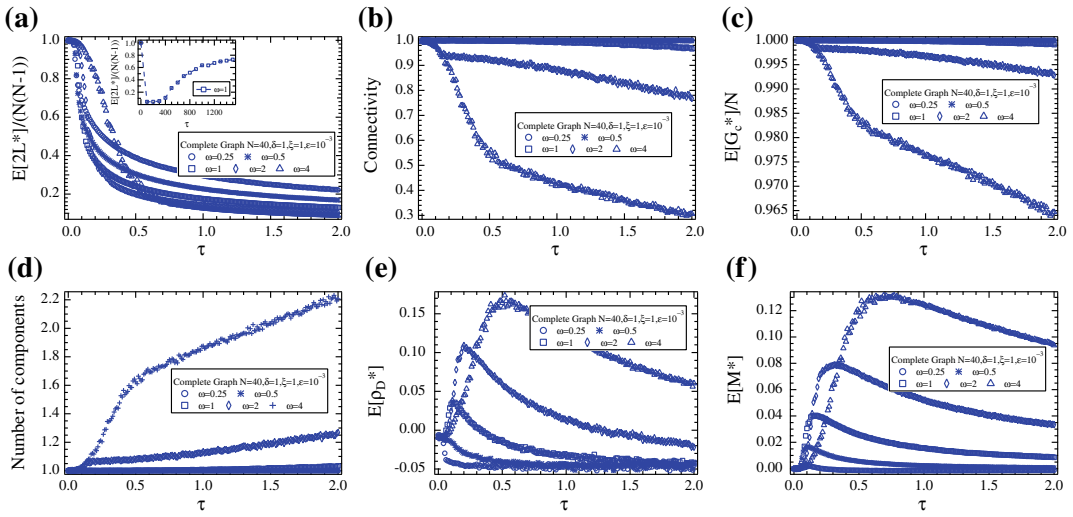

Fig. 8.5 (Color online) The effect of the effective infection rate τ on the topology in the metastable state. **a** $\frac{E[2L^*]}{N(N-1)}$ the average number of links in the metastable state scaled by the maximum number of links ($\frac{N(N-1)}{2}$ in a complete graph) as a function of τ. The effect of large values of τ is shown in the inset. **b** The probability of the graph being connected in the metastable state as a function of τ. **c** $\frac{E[G_c^*]}{N}$ the normalized average size of the biggest component in the metastable state as a function of τ. **d** The average number of components in the metastable state as a function of τ. **e** Assortativity value on average $E[\rho_D^*]$ in the metastable state as a function of τ. **f** Modularity value on average $E[M^*]$ in the metastable state as a function of τ

The Effect of the Link Dynamics on the Topology in the Metastable State

In a similar way, all these metastable stable network properties can be shown in relation to the effective link-breaking rate ω, which characterizes the link dynamics. It has been observed that as ω increases, the network becomes sparser, disconnected with a higher probability into more components, both the assortativity and modularity increase first and decline afterwards. More details can be found in [118].

Structure of the Topology in the Metastable State

Figure 8.6b presents an overview of the modularity as a function in effective rates τ and ω for $\delta = 1$ and $\xi = 1$. The modularity in the ASIS model is high and it appears to show "half-open", "elliptical-like" curves. The explanation behind high modularity lies in the fact (a) there is a clear separation between the susceptible and infected nodes and (b) the sizes of the S and I components are similar. This can be explained as follows. A high modularity means (i) that the infected nodes and the susceptible nodes are well separated, and (ii) that the I component is comparable in size to the S component. Such high values of modularity can be achieved for moderate values of τ and ω such that the epidemic can be spread it fast enough (the role of high enough/moderate τ) and it will not be suppressed (the role of moderate ω) and this can be achieved for several values of τ and ω thus forming "half-open", "elliptical-like" curves. On the other hand, similar low values of modularity can be achieved for either small τ with high ω or high τ with small ω. In the former, the epidemic spread is

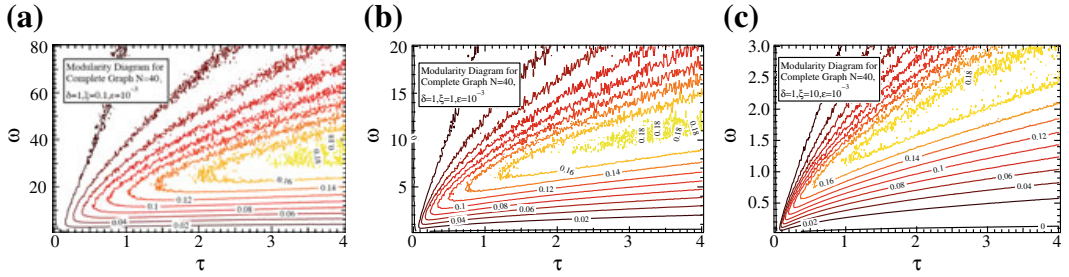

Fig. 8.6 (Color online) The contour lines of the modularity contours depending on τ and ω for three different values of link-creating rate ξ: **a** $\xi = 0.1$, **b** $\xi = 1$, and **c** $\xi = 10$

negligible and will be suppressed fast enough, thus leaving noticeable S component; while in the later the epidemic is spread very fast and cannot be suppressed, thus forming significant I component. Both cases lead to similar low modularity values also forming wider "half-open", "elliptical-like" curves. The connectivity also shows very similar "half-open", "elliptical-like" curves in a plane with τ and ω dependence, but opposite to modularity i.e. high connectivity leads to low modularity and *vice versa*. The degree distribution for the all nodes and separately for the infected and susceptible nodes have been discussed in more details in [118]. It has been shown that when the infection process is faster than the link dynamics, the final degree distribution is binomial-like, while in the opposite case there are multiple peaks in the degree distribution.

Determing the Bi-Stability in the ASIS Model

We explore the distribution $\Pr[Z^*]$ of the fraction Z^* of infected nodes in the metastable-state instead of the average $y = E[Z^*]$. Figure 8.7 shows the $\Pr[Z^*]$ for diverse effective infection rates τ and fixed link dynamic rates ξ and ζ. When $\tau = 0.15$ is low, the meta-stable state approaches the healthy state. When $\tau = 3$ is high, the meta-stable state is the endemic state. The fraction Z^* of infected nodes in the meta-stable state is either close to 0 or a non-zero positive value for some other cases (for example, the $\tau = 1$ case in Fig. 8.7). When $\tau = 1$, the probability $\Pr[Z^* = 0]$ approximates the probability $\Pr[Z^* = c]$), where c is positive and dependent on τ. This implies that the metastable state is likely stable at the two dramatically different infection states, a seemingly bi-stability phenomenon. Such phenomenon in epidemic spreading on adaptive networks was reported by Gross et al. in [116]. The bistable state is a metastable state where the infection persists or there is no infection in the ASIS model.

A bifurcation-like behavior is illustrated in Fig. 8.8. The probability $\Pr[Z^* = 0]$ is comparable with the probability $\Pr[Z^* = c]$ for a certain τ in value. The metastable state of the ASIS model is possibly stable in either of the two states. It seems that the metastable state changes from the healthy state, to the bi-stable state and to the endemic state as τ increases.

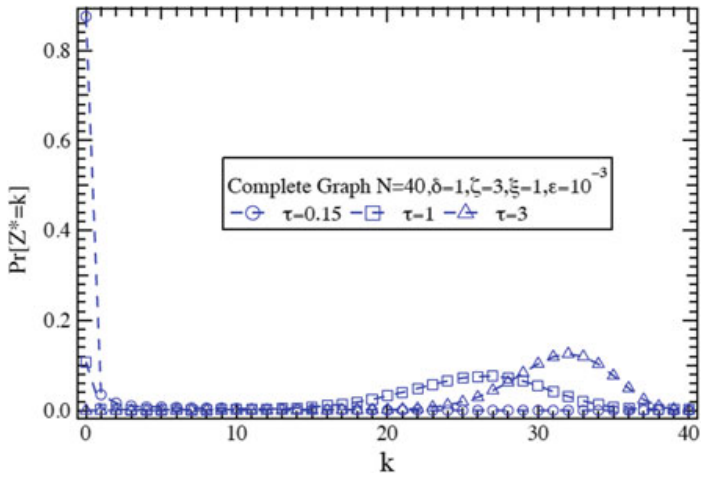

Fig. 8.7 (Color online) The fraction of infected nodes Z^* in the metastable state

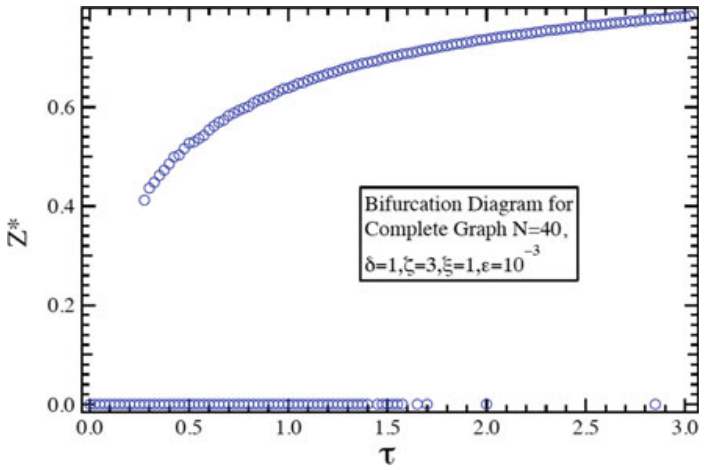

Fig. 8.8 (Color online) The bifurcation diagram of the fraction of infected nodes in metastable state. The metastable state is the healthy state when the effective infection rate $0 \leq \tau \leq 0.3$), the bi-stable infection state when $0.3 \leq \tau \leq 1.6$ and the endemic state when $\tau \geq 1.6$ in sequence as τ increases

8.1.4 Summary

We proposed an adaptive network model *ASIS* to characterize the interplay and co-evolution between the dynamics on a network (e.g. disease spreading) and the dynamics of the network (i.e. dynamics of the link state). This model includes a Poissonion link-breaking process with rate ζ and a Poissonion link-creating process with rate ξ in the classic Susceptible-Infected-Susceptible (SIS) model. When the initial topology of an adaptive network is a complete graph, the average fraction of infected nodes in metastable state has been derived (see Theorem 8.1). Moreover, we have proved and illustrated a linear law between the epidemic threshold τ_c and the effective link-breaking rate $\omega = 2\zeta/\xi$ We have also verified experimentally (see Theorem 8.2) that the phase transition that a disease can persist in the presence of link dynamics for the effective infection rate $\tau > \tau_c$, and the linear function $\tau_c(\omega)$.

Our simulations point out how the co-evolution of the disease and link dynamics promotes the emergent features of the adaptive network with respect to the connectivity, the number of links, the biggest component size, the associativity and modularity . Nodes group into two loosely inter-connected clusters according to their viral

states, i.e. the I (infectious) component and the S (susceptible) component, based on which the modularity is calculated. When the disease dynamics is faster than the link-breaking process and the link-creating process in rate, the network evolves towards no apparent community structure and disassortative-mixing. When the epidemic spreading is slower than the link dynamics, the topology becomes slightly but clearly modular and assortative. A universal contour-line pattern can be observed in the modularity diagram as a function of τ and ω. A high link-breaking rate ω or a low infection rate τ may lead to disassortative networks with low modularity. In contrast, a low connectivity tend to contribute to a high modularity in network topologies.

Finally, our investigation on the distribution of the fraction of infected nodes in the metastable state shows that between the healthy state and the endemic state, a bi-stable state may exist where the fraction of infected nodes is stable either around 0 (the healthy state) or around a positive non-zero value (the endemic state).

8.2 Comparison of the ASIS and AID Model

8.2.1 The AID Model

Both the ASIS and AID are based on the SIS epidemic spreading model. However, the dynamics of the topology evolution in these two coevolution models are opposite. The Poissonian *link-breaking* and *link-creating* processes with rates ζ and ξ respectively, govern the evolution of the network topology. In the AID model, a link is created between a node pair when only one node but not both has the information. An existing link is removed between a node pair, when both nodes do not have the information, and if the two nodes were not connected in the original network. For the link existence probability $E\left[a_{ij}\,(t)\right] = \Pr\left[a_{ij}\,(t) = 1\right]$, we have the following governing equation

$$\begin{aligned}\frac{d}{dt}E[a_{ij}] =&(1 - a_{ij}\,(0))E\Big[- \zeta a_{ij}(1 - X_i)(1 - X_j)\\ &+ \xi(1 - a_{ij})\left(X_i - X_j\right)^2\Big].\end{aligned} \tag{8.9}$$

We consider the simple case where the initial network is an empty graph with N isolated nodes and without any link. When both i and j have the information ($X_i = X_j = 1$), the link is preserved, i.e. $\frac{dE\left[a_{ij}\right]}{dt} = 0$. The link dynamics, thus, tend to increase (decrease) the degree of a node with (without) information.

The AID model has be verified to be realistic by using the Facebook wall posts dataset [117].

Table 8.1 Comparison of AID and ASIS models

Property/model	ASIS	AID
Metastable state	Always stable	Unstable (τ, ω) regions
Threshold $\tau_c(\omega)$	Linear	(mostly) constant
Topological metrics	"half-elliptical"	Rotated "half-elliptical"

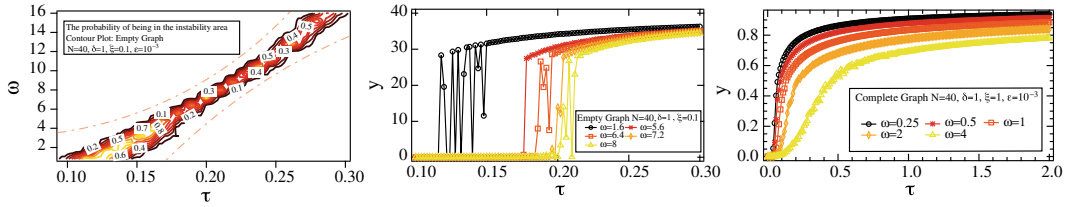

(a) Instability region for the AID model.

(b) The prevalence y in the AID model.

(c) The prevalence y the ASIS model.

Fig. 8.9 **a** and **b** demonstrate the instability in AID. **c** demonstrates the stability in ASIS

8.2.2 Comparison

We are going to illustrate the striking difference that emerges from AID and ASIS. The most important difference is that instability and non-existence of the metastable state are observed in the AID but not the ASIS model. Key differences between the two models are given in Table 8.1, which will be further explained.

8.2.3 The Prevalence

Exact expressions for the fraction of infected nodes and the epidemic threshold for the AID model has as well been derived in [117]. Although these relations are not of closed-form, they can well explain the existence of the metastable state and the stability of the prevalence for both models. We denote the prevalence in the metastable state by $Z^* = \frac{1}{N}\sum_{j=1}^{N} X_j^*$ and its average by $y = E[Z^*]$ where N is the number of nodes in the network. We further denote $T(N) = \frac{E\left[\sum_{i=1}^{N} d_i^*(1-X_i^*)\right]}{N^2}$, which is bounded by

$$0 \leq T(N) \leq \frac{E\left[\sum_{j=1}^{N} d_j^*\right]}{N^2} = \frac{E[2L^*]}{N^2} \leq \frac{N(N-1)}{N^2} < 1.$$

In the AID model,

$$y = \frac{1}{2}\left(1 + \frac{\omega - 2}{2\tau N}\right)\left(1 \pm \sqrt{1 - \frac{4\mathrm{Var}\left[Z^*\right] + 2\omega T(N)}{\left(1 + \frac{\omega-2}{2N\tau}\right)^2}}\right), \tag{8.10}$$

where $\mathrm{Var}[Z^*]$ is the variance of the prevalence and d_j^* is the degree of node j. Importantly, the argument under the square root in (8.10) is possibly negative, leading to the **non-existence** of the metastable state. Consider a large network, where $N \to \infty$. In this case, (8.10) can be simplified to

$$y = \frac{1}{2}\left(1 \pm \sqrt{1 - \left(2\omega T_\infty + 4\mathrm{Var}\left[Z^*\right]\right)}\right). \tag{8.11}$$

The metastable state does not exist, if $4\mathrm{Var}\left[Z^*\right] + 2\omega T_\infty > 1$. Therefore,

$$\mathrm{Var}\left[Z^*\right] > \frac{1}{4}$$

is sufficient to lead to the non-existence of the metastable state. Furthermore, an upper bound for the link-breaking rate can be derived from (8.11):

$$\omega \leq \frac{1 - 4\mathrm{Var}\left[Z^*\right]}{2T_\infty} \leq \frac{1}{2T_\infty},$$

otherwise, a metastable state solution does not exist. These findings in theory are confirmed by simulations. As shown in Fig. 8.9a and b, the metastable state does not exist in certain regions of (τ, ω). The **instability area** reveals a "sand clock" shape: as τ and ω increase, the area narrows first and then widens. The area vanishes for large enough τ and ω.

In contrast, the metastable state always exists in the ASIS according to (8.7).

Consider the combination of all the four parameters of the AID model. When the link breaking rate is higher than the creating rate but both are large and the spreading rate is small, a small fraction of nodes possessing the information are unlikely to stay long nor can be considered as a metastable state. In this case, both the number of links and infected nodes change dramatically over time, as shown in Fig. 8.10a. Whereas in other combinations of the parameters, there is usually a critical mass of links and nodes that possess the information, forcing of the epidemic to reach an equilibrium, i.e. the metastable state (see Fig. 8.10b).

8.2.4 *Epidemic Threshold τ_c*

We have shown that the epidemic threshold (8.8) in the ASIS model is linear in ω.

The threshold in the AID model is, however, the quotient of two linear functions, which approaches a constant if ω is large,

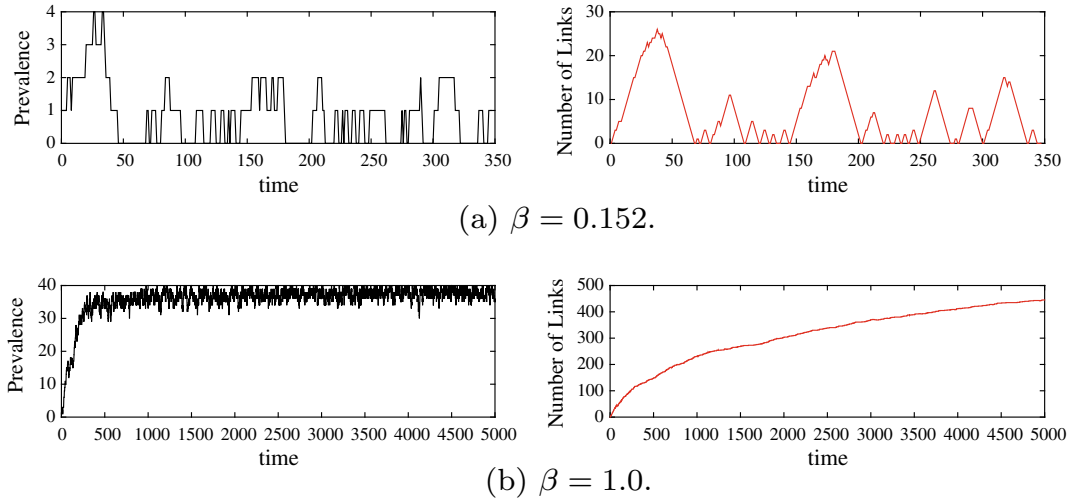

Fig. 8.10 (Color online) The numbers of links and infected nodes as functions of time in the AID model, where $N = 40$, $\zeta = 0.32$, $\xi = 0.1$, $\delta = 1$, $\varepsilon = 10^{-3}$ and different spreading rates β are considered. The points of instability/stability are in accordance to Fig. 8.9a

Fig. 8.11 (Color online) Threshold τ_c versus effective link-breaking rate ω for $N = 40$ (the inset: large range of ω)

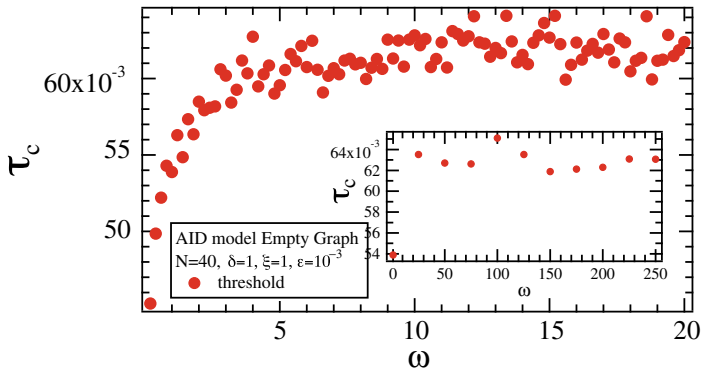

$$\tau_c(\omega;\xi) = \frac{\omega - 2}{2N\left(h_{\mathrm{AID}}(\omega;\xi) - 1\right)}, \tag{8.12}$$

where $h_{\mathrm{AID}}(\omega;\xi) \leq 1 + \max\{1, 1 + \frac{\omega-2}{2Na}\}$ and $a = \lim_{\omega\to\infty} \frac{\partial h_{\mathrm{AID}}(\omega;\xi)}{\partial\omega}$ is approximately a constant. If $\omega > 2$, $h_{\mathrm{AID}}(\omega;\xi)$ is almost a linear function of ω, obeying $h_{\mathrm{AID}}(2;\xi) = 1$.

Figure 8.11 illustrates the relation between the epidemic threshold and ω and the epidemic threshold is almost a constant when ω is large. The epidemic threshold in Fig. 8.11 is relatively noisy, a fingerprint of the instability in the AID model.

8.2.5 *Topological Properties*

Figure 8.12 depicts the contour plot of the network modularity in the metastable state in the (τ, ω)-plane, for both ASIS and AID models. Interestingly,for a given effective

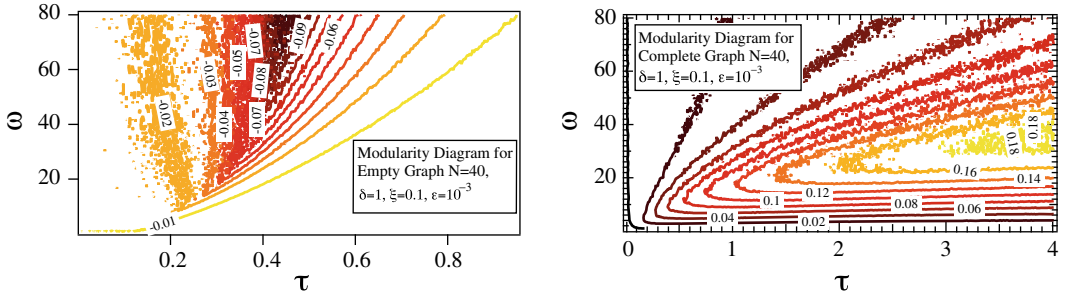

(a) AID model. (b) ASIS model.

Fig. 8.12 (Color online) Modularity in (τ, ω)-plane in the stable region for $\xi = 0.1$

infection rate τ, small and large effective link-breaking rates ω may lead to the same modularity. The ASIS and AID models differ in the order of the contour lines: "the inner contour" lines show higher (lower) modularity in ASIS (AID) but have similar shape, though rotated, in the contour lines.

In the (τ, ω)-plane, the instability area, which has "sand-clock" shape (Fig. 8.9a), exists only The instability area for the AID model, is close to the center of the coordinate system in the (τ, ω)-plane and bellow the "half-ellipses" extremal node.

The *metastable state* (when it exists) topologies in the AID model are random graphs. In the metastable state of the ASIS model, the networks have, however, two clusters that are sparsely connected. One cluster is composed of the susceptible nodes, which are almost fully connected and the other is composed of the infected nodes, connected like a random graph.

8.3 Conclusion

The two process and network coevolving models ASIS and AID share the same epidemic spreading process but different topology dynamics. Via our theoretical analysis and extensive simulation, we have observed and explained their differences from the following perspectives:

1. Instability of the metastable state exists in the AID but not the ASIS model.
2. The epidemic threshold τ_c tends to be independent of the effective link-breaking rate ω when ω is large in the AID model, whereas linearly increases with ω in the ASIS model.
3. Topological features such as the modularity of both models exhibit concentric half-ellipses in the (τ, ω)-plane. The two models differ in the order rotation of the contours.